Inducing Knotted Defect Structures in Nematic Liquid Crystals via Boundary Conditions

By: Zachary Winoker

Advisor: Robert Pelcovits

Final Draft

May 3, 2013

Abstract

Simulations are an important tool in contemporary liquid crystal research. They provide the means to study the relationship between microscopic molecular orientation and macroscopic traits.

A common model employed in liquid crystal simulations is the Lebwohl-Lasher model [7]. In it, nematic liquid crystal molecules are modeled as rods affixed to points on a cubic lattice. These rods interact with each other through a nearest-neighbors pairwise potential [7]. Monte Carlo simulations have recently been used to investigate the effects of electric fields on the Lebwohl-Lasher model's equilibrium configurations.

In this project, we use Monte Carlo simulations of the Lebwohl-Lasher model to study knotted configurations of defect lines in nematic liquid crystals. Defect lines are an orientational irregularity that can appear at equilibrium in nematic liquid crystals under specific boundary conditions [2, 3, 7, 8]. We attempt to find a boundary condition that either produces a knotted defect structure by itself or does so in tandem with another time-dependent boundary condition.

We hypothesize that two methods of production are possible for the generation of knotted defect structures. The first method is to spontaneously generate a structure equivalent to a Hopf link, which is a pair of circles linked together exactly once [19]. The second approach is to create a topologically stable unit knot, which is one circle [19]. If the unit knot can be created, we hypothesize that multiple unit knots can be linked or knotted using manipulations of the boundary conditions. We employ two variations of the latter method, one using an orthogonal pair of the boundary conditions described by Backer [6] and another using a wedge disclination loop [18].

For the Hopf link method, we employ time-independent and time-dependent variations on the boundary conditions used by Backer (hereafter referred to as Backer boundaries). The results are currently inconclusive for this attempt.

The unit knot method failed to produce knotted defect structures. We believe that the

combination of Backer fields fails due to relationships between side length ratios and defect line formation between Backer boundaries. The wedge disclination loop (hereafter called WDL) method fails due to the loop's high degree of instability under Backer boundaries. Variations on these methods are suggested in this paper's penultimate section.

These simulations are based on studies of chiral nematic colloids by Tkalec *et al* [17]. In these studies, laser tweezers were used to manually link together arbitrary numbers of Saturn Rings. So far, our results indicate that similar behavior is not observable in nematics using electric field manipulation.

Introduction

States of matter are usually classified by the types and degrees of order they possess. Two of the most common states are crystalline solids and isotropic liquids. Most materials transition directly between these two states as they are either heated or cooled. However, there is a class of materials that pass through intermediate phases known as liquid crystal phases. As the name suggests, these states are neither entirely crystalline or entirely liquid in nature. In general they are more ordered than a liquid and less ordered than a crystal. The former has no positional or orientational order while the latter has both. Liquid crystals have some degree of orientational order and may have some degree of positional order.

The molecules in a liquid crystal are roughly shaped like either rods or discs. Left alone, they will align in a particular direction. This direction depends on the intermolecular potential associated with a given material.

The simplest liquid crystal phase is the nematic phase. Many nematic liquid crystals have long, thin, and stiff molecules which allows them to easily be approximated as rigid rods. These molecules exhibit the strongest attractive force when aligned parallel to one another, and will therefore all align in the same direction if left to equilibrate. This preferred direction is represented by a vector field called

the director field. For a nematic, the director field has a symmetry whereby it is invariant under a 180 degree rotation [16].

Singularities in the director field, called defects, can arise from fixed boundary conditions on a liquid crystal. These boundary conditions disrupt the director field's uniformity and can cause novel irregularities in the nematic's bulk. The boundaries can be generated by exposing the surface of a liquid crystal cell to an optical lattice or a magnetic field, or by other means. In this project, we explore the use of boundary conditions in generated knotted defect structures.

Knots

A knot is an embedding of a circle in 3D Euclidean space. Likewise, a link is an embedding of at least 2 circles in 3D Euclidean space. Two knots or links are identical if they can be transformed into one another using Reidemeister moves. These moves are operations on a knot corresponding to twisting, lifting and moving, or moving over a crossing, all of which are illustrated below [19].

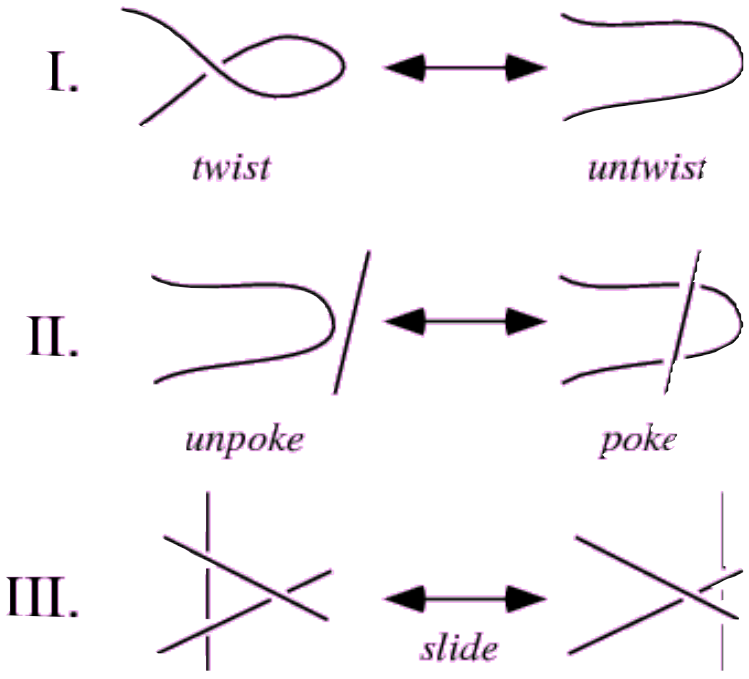

Figure 1: The Reidemeister moves indicate which actions can be performed on a knot without changing its classification. Note that knots cannot be cut or glued together in any of these moves [5].

The fundamental knot is simply a circle, known as the unknot. The unknot can be used to construct more complicated knots and links. For example, two unknots can be used to construct a Hopf Link. To do so, one unknot must be cut and then re-glued together such that it is linked with the other unknot. Since this is the only way to make a Hopf Link from two unknots, the unknot is not in the same class as the Hopf Link.

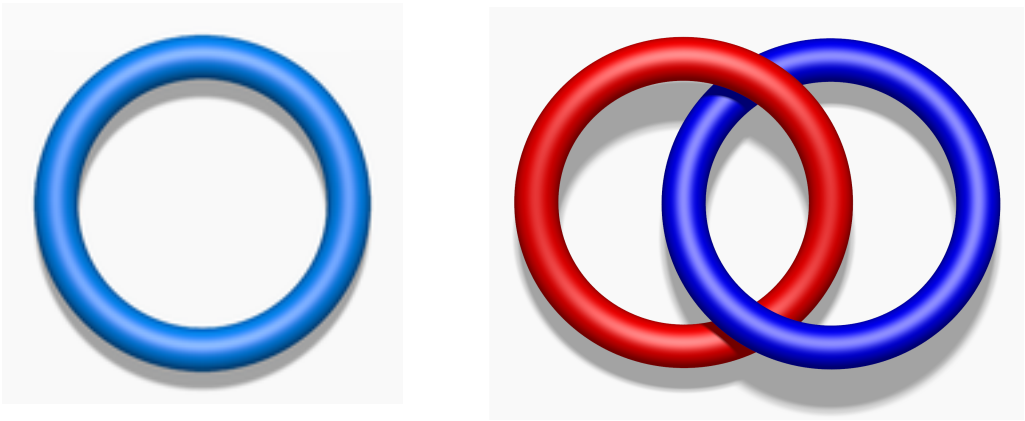

Figure 2: On the left is the simplest knot, the unknot [4]. *It is equivalent to a circle and is also called the trivial knot. On the right is a Hopf Link, the simplest link* [1]. *It is equivalent to two unknots linked together exactly once.*

In our attempts to create knotted defect structures, we use non-Reidemeister moves on disclinations, which are described in the section of the paper titled **Defects**.

Background

Order Parameter

Maier and Saupe provided a theory of the nematic phase in which they describe the alignment of molecules relative to a preferred direction using an orientational order parameter [16]. Using the mean field approximation, they derived that there is an attractive potential proportional to

$$-(3/2)cos^2(\theta_{ij}) - (1/2)$$

between molecules in the nematic phase. Here, Θ_{ij} is the angle between the long axes of two different molecules.

If the preferred direction is not known, the following rank 2 tensor is used to determine a scalar order parameter:

$$Q_{ab} = (1/N_m)\sum_{i=1}^{N_m}[(3/2)(\hat{u_{ia}} \cdot \hat{u_{ib}}) - (1/2)\delta_{ab}]$$

where δ_{ab} is the kronecker delta, the $\hat{u_{ia}}$ are the components of a molecule's orientation vector, and N_m is the number of molecules. The sum is taken over all molecules.

We can diagonalize Q_{ab} and find it has eigenvalues related by :

$$\lambda_{-1}=\lambda_0=-(½)\lambda_{+1}$$

We then take the order parameter S to be λ_{+1}. Then the director field is given by the eigenvector associated with λ_{+1}.

However, if we know the preferred direction then we can use a scalar order parameter:

$$S=<P_2(\cos(\Theta))>=<(3/2)\cos^2(\Theta)-(1/2)>$$

where theta is the angle between the long axes of a given molecule and the preferred direction and $P_2(x)$ is the second Legendre polynomial.

Note that for a sample with completely random orientations, the order parameter is 0. If all molecules point in the same direction, then the order parameter is 1.

Defects

In a neutral environment, an achiral nematic liquid crystal is the most stable when all of its molecules are aligned in one direction [7]. Certain external conditions, such as applied boundary conditions, can disrupt this alignment such that the director field discontinuously changes at a point. These discontinuous changes are called defects, and the director field is undefined at their location.

If the director is undefined at a single point, the liquid crystal is said to contain a point defect. If the director is undefined along a curve, then the liquid crystal is said to contain a line defect, also called a disclination. At disclinations and point defects, the Frank free energy density diverges and is finite elsewhere.

We classify disclinations and defect points by their discontinuous change in the director field [8, 16]. These changes are identified by a number and a sign. The number represents the angle through which the director rotates across the defect (e.g. 1/2 for a 180 degree rotation). If two defects have the opposite sign and same magnitude, then they can annihilate one another. That is, their superposition will result in a defect of strength (i.e. number) 0, which is equivalent to the absence of a defect.

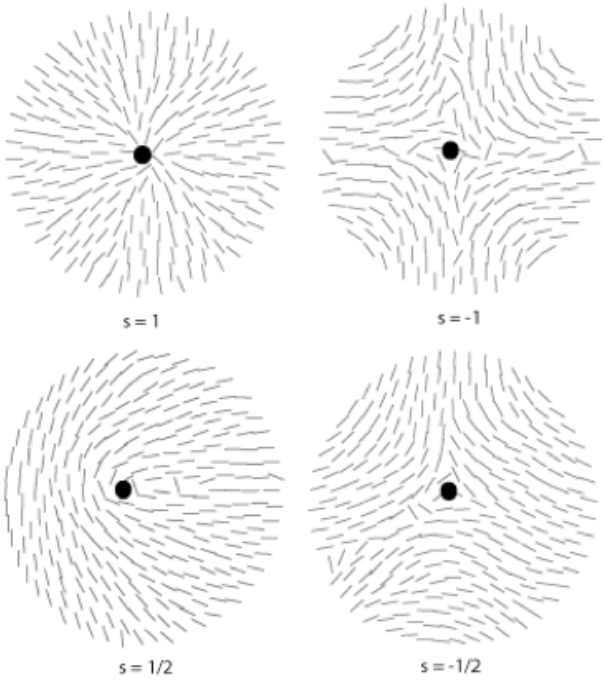

Figure 3: Examples of disclinations in a nematic liquid crystal. The dot indicates the location of the defect and the lines indicate the orientations of nearby molecules.

It is possible for a system with integer strength defects to relax to a defect-free configuration. This is accomplished by a continuous rotation of the director field out of the plane containing the defect and its surrounding molecules [7]. This process is called “escaping into the third dimension,” and demonstrates that integer strength defects are not stable, since the rotation eliminates the defect.

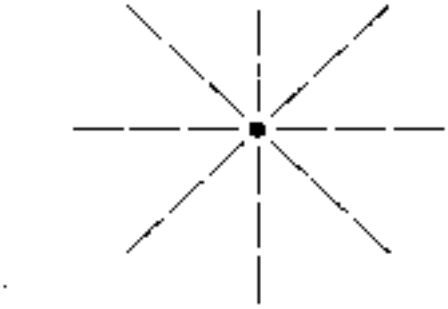

Figure 4: A 360 degree defect, also called a defect of strength 1. This defect is topologically unstable because the director rotates around it by an even multiple of 180 degrees.

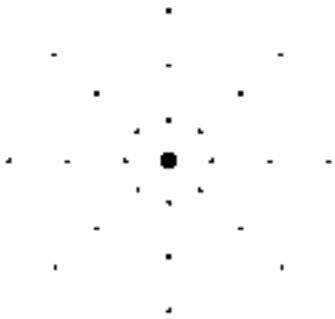

Figure 5: Here, we've let the 360 defect escape into the third dimension. A continuous rotation of the director field around the defect has resulted in the director being every perpendicular to the page.

Conversely, half-integer strength defects are stable in a nematic. Note that any attempt to

continuously escape into the third dimension will leave a singular line extending outward from the defect center. Therefore, the configuration containing the defect point is energetically favorable.

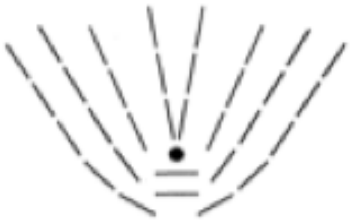

Figure 6: This defect is topologically stable since the director rotates around it by 180 degrees.

We discuss topological stability of defects and the process of detecting them in the methods section of this paper.

Defect Structures

Our attempts to generate knotted defect structures employ two other well-understood defect structures. In particular, we use boundary conditions that generate what we call Backer lines (as they are due to Backer) and those that generate a Wedge Disclination Loop (WDL).

Backer lines are a pair of 1/2-integer strength disclinations that are generated by the following boundary conditions [6]:

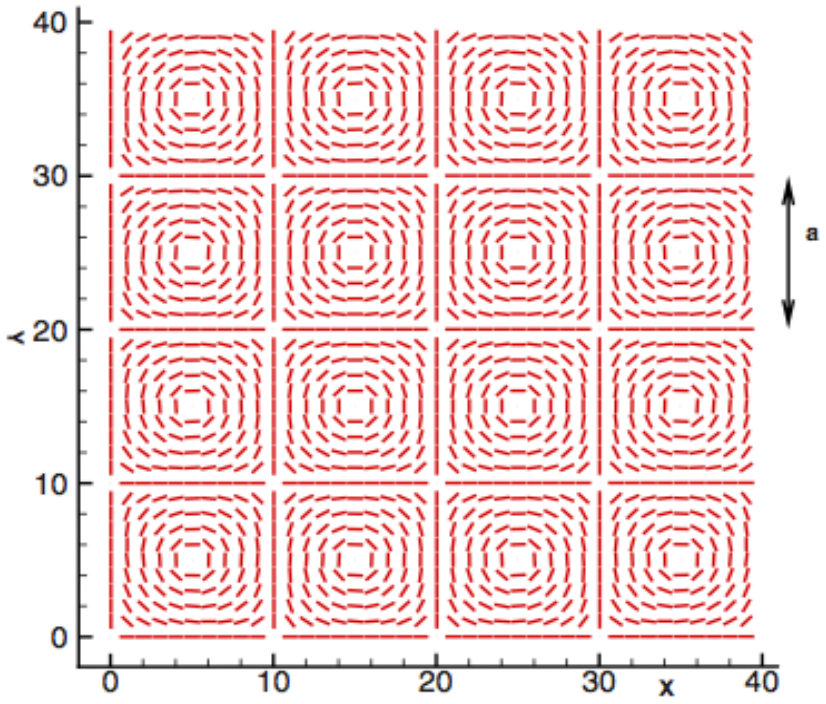

Figure 7: The boundary conditions used in Backer's simulations.

Note that the center of each Backer cell is a defect of strength -1 and each corner is a defect of strength 1. Backer et al found that a pair of 1/2-integer disclinations formed between the -1 defect points once the sample had equilibrated. As such, Backer boundaries provide a reliable and easy way to generate 1/2-integer disclinations, which are a key ingredient in our proposed knotted structures.

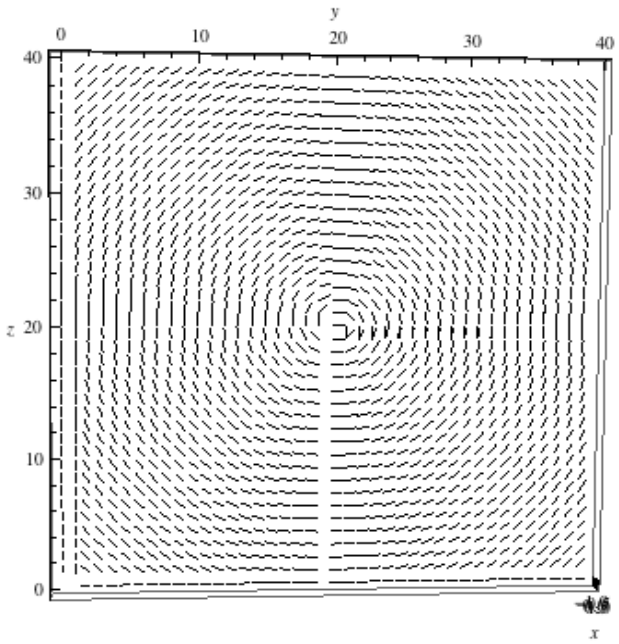

Figure 8: In the approach detailed in this section, a boundary was composed of a single Backer cell, as shown above. Note that the slanted profile is an artifact of the graphing software used for this image.

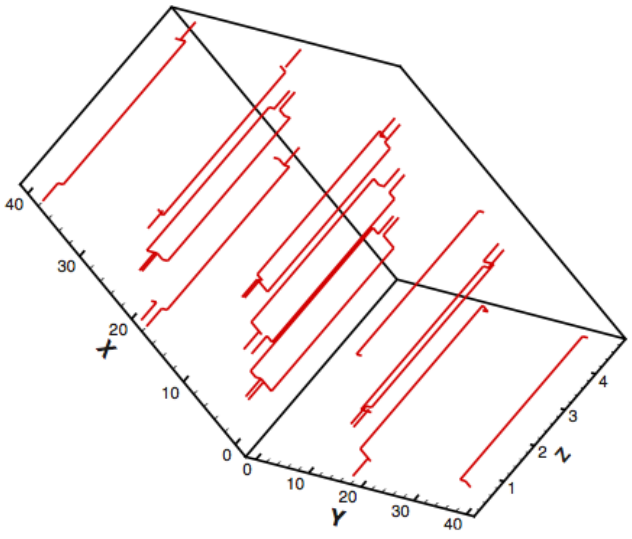

Figure 9: A pair of 1/2-integer disclinations connects each defect of strength -1 on opposing Backer boundaries.

The Wedge Disclination Loop is a circular 1/2-integer disclination that is generated by radially outward pointing boundary molecules. These boundaries mimic the electric field of a monopole, which results in a "pinching" of the director field in a circular region around the center of the sample. We use this loop in order to create a unit knot, which is our fundamental structure [18].

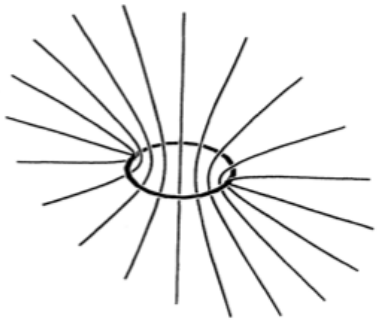

Figure 10: A wedge disclination loop and the surrounding director field

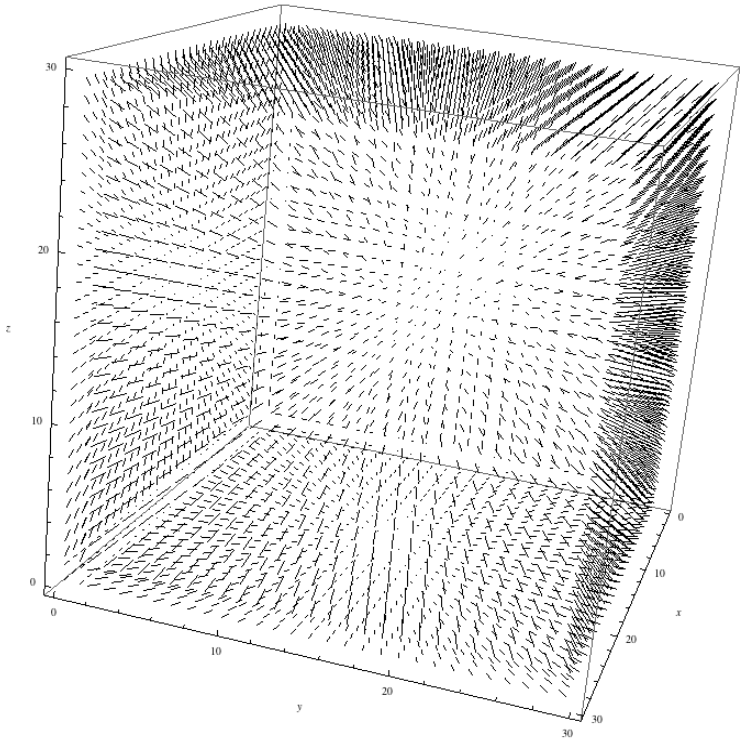

Figure 11: The boundaries used to create a WDL point radially outward.

Motivating Experiments

Our methods are inspired by experiments performed by Tkalec et al. In these experiments, knots and links of arbitrary complexity were constructed in chiral nematic liquid crystals [17]. These knots were assembled as follows. First, specially treated silica microspheres were placed in a chiral nematic liquid crystal (CNLC). These spheres were chemically functionalized such that nearby CNLC molecules aligned normal to their surfaces. Each of these spheres acquired a single disclination loop that encircled its equator. This loop is known as a Saturn's ring and is topologically equivalent to the unknot. Using optical tweezers, multiple spheres were brought together. Their Saturn's rings then either spontaneously fused or were encouraged to do so by melting the rings' contact points with a laser. By linking and fusing unknots like this, Tkalec et al were able to create arbitrarily complex defect structures.

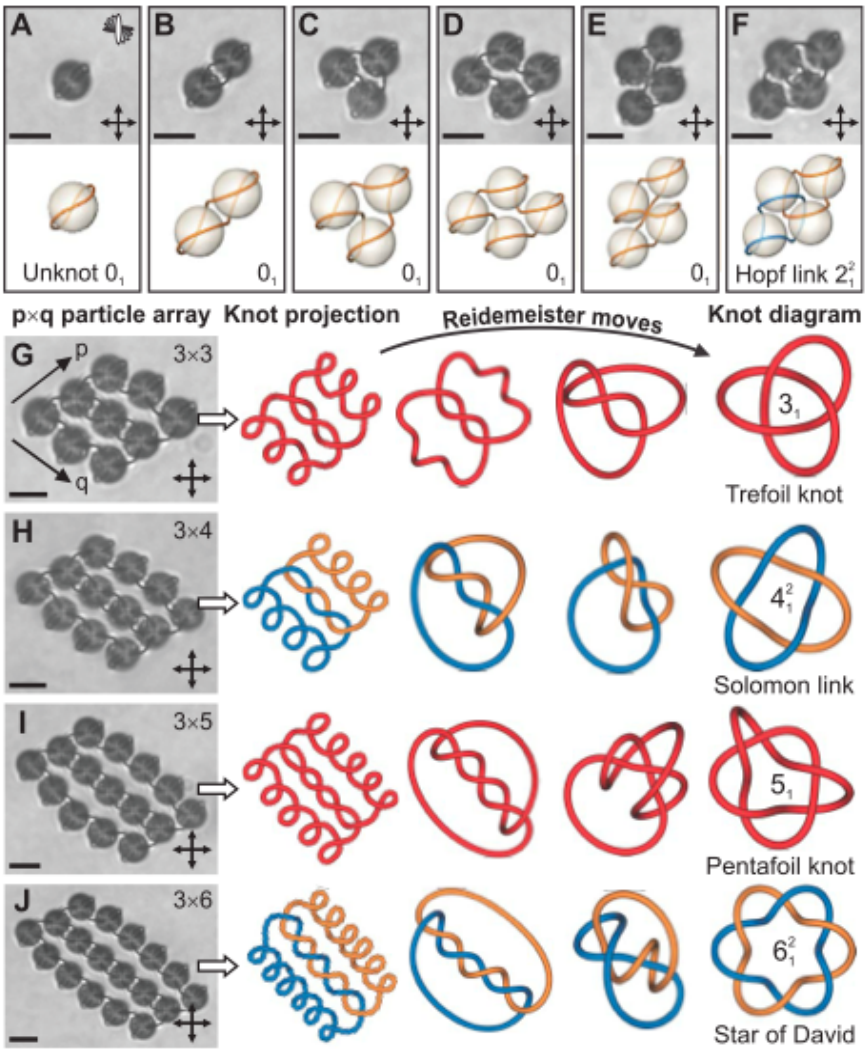

Figure 12: By manipulating specially treated microspheres with optical tweezers, Tkalec et al. were able to create knotted defect structures of arbitrary complexity.

In our simulations, we used achiral nematic liquid crystals instead of chiral nematic liquid crystals. This is due to the comparative simplicity of achiral nematics, the well-understood and available boundary conditions on nematics, and similar experimental work on nematics by Ravnik et al again using colloidal spheres [12].

We aim to create a boundary-induced structure similar to the Saturn ring. We would like to

adjust boundary conditions in order to move this structure in the same way that optical tweezers are used to move Tkalec's microspheres. This will allow us to move unknots close to each other and see if they can be linked either spontaneously or via perturbations in the boundary conditions. In this way, we hope to be able to create knots of arbitrary complexity using only boundary conditions.

Why Boundary Conditions?

Tkalec's method is thorough and very flexible, but difficult to scale due to its manual nature. We asked if it was possible to create similar structures using a more automated method. The natural choice for such a method was boundary condition manipulation induced by electric fields. This approach, if effective, would allow for the creation and manipulation of knotted defect structures using automatically generated and modified electric fields applied to liquid crystals. The experimental implementations of this method are also very flexible. That is, if a field appeared to generate the desired structures, it could very likely be created in the lab. Therefore, the results of our simulations would be immediately testable.

We use boundary conditions because the electric fields in question anchor the outermost layers of a liquid crystal into a specific configuration [6]. So by fixing the boundaries of a liquid crystal in a specific pattern, we effectively simulate the action of an electric field.

Notes on Our Simulation

Lebwohl-Lasher Model

We use Monte Carlo simulations of the 3-dimensional Lebwohl-Lasher model to test our hypothesis. In the Lebwohl-Lasher model, liquid crystal molecules are approximated as rods. Each rod is affixed to a point on a cubic lattice, where it is free to rotate in all directions but not to move between lattice points [16]. Despite the model's simplicity, it accurately reproduces the orientational ordering of

nematic liquid crystals at equilibrium.

Our lattices had cubic unit cells and had varying height/width/length ratios. Our largest simulations were 100 x 100 x 100 lattice points, although most had side lengths less of than 60 points due to restrictions on computational power.

The total energy of the simulation is calculated by computing the sum of nearest-neighbor pairwise interactions in the lattice. These pairwise interactions are dependent only on the relative orientations of molecules' long axes. This interaction is, for the nematic phase,

$$Energy = -J(\hat{u}_i \cdot \hat{u}_j)^2$$

Where J is the maximum interaction energy and $\hat{u}_i$, $\hat{u}_j$ are unit vectors parallel to the two molecules' long axes. Clearly this potential favors parallel molecules, as a parallel configuration would produce the largest dot product and thereby the lowest energy since the coefficient J is positive. The potential energy associated with a single molecule is the sum of this pairwise interaction over its nearest neighbors. The total energy of the system is then just the sum of each pairwise potential.

Monte Carlo Algorithm

To drive this system towards equilibrium, we employ a Monte Carlo algorithm. This algorithm simulates the disordering effect of non-zero temperatures on a molecular ensemble. In particular, it brings the ensemble into equilibrium with a constant heat source of temperature T.

In this algorithm, the orientations of all non-boundary molecules are initially randomized. Next, a random molecule is selected. Its orientation is randomized, and then its energy contribution is recalculated. If the new orientation lowers the system's overall energy, then it is kept. Otherwise, the new orientation is kept with a probability equal to the following ratio of Boltzmann factors:

$$e^{((E_n - E_p)/kT)}$$

Here, E_n is the energy with the new orientation, E_p is the energy with the previous orientation, k is the Boltzmann constant, and T is the temperature of the heat bath.

Over time, this process will drive the system towards an equilibrium configuration. An equilibrium configuration is defined as one where repeated Monte Carlo iterations will not reduce the number of defects. At equilibrium, the energy of the system is minimized and the order parameter is maximized.

Defect Finding Algorithm

After the system equilibrates, we search for 1/2-integer defects using a defect finding algorithm. We choose 1/2-integer defects because backer boundaries generate 1/2-integer disclinations, which also lower the energy, so we should expect to find them in our samples. The following defect algorithm, due to Zapotocky, Goldbart, and Goldenfeld, is run on each point in the lattice. We first take the molecule located at lattice point (x, y, z). The vector identified with the molecule's orientation is dotted with the corresponding vector at (x, y + 1, z). If the result is negative, we create a copy of the molecule at (x, y + 1, and z) and rotate it 180 degrees so that the dot product is negated. We do the same for (x, y + 1, z) and (x, + 1, y + 1, z). Then we repeat the process for the lattice points (x + 1, y + 1, z) and (x + 1, y, z). Finally, we dot the copy of the molecule at (x + 1, y, z) with the rod at (x, y, z). If this last dot product is negative, then there is a 1/2-integer defect located in the cell bordered by these four points. We do the same for loops in the YZ and XZ planes. Note that if the process is repeated for each lattice point, we only need to consider loops in the positive directions in order to cover all possible cells (i.e. x to x + 1 instead of x to x – 1) [9].

This algorithm successfully finds 1/2-integer defect points due to a topological property of the order parameter space for uniaxial nematics. For this type of liquid crystal, there is only one type of stable point defect, the 1/2-integer defect (AKA the 180 degree defect) [8]. Consider this defect and an integer (360 degree) defect, pictured in a previous section. We can trace a loop around each point and

draw a corresponding loop in the order parameter coset (OPC) space, which is topologically equivalent to the projective plane. Pictured below are the loops in OPC space corresponding to an integer and half-integer defect point below. Note that for the integer defect we generate a contractible loop in OPC space and for the half-integer defect we generate a non-contractible loop.

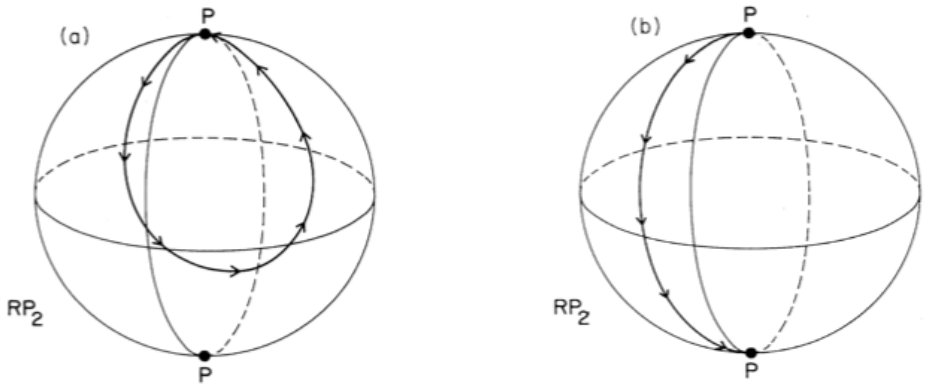

Figure 14: A contractible loop (left) and non-contractible loop (right) in uniaxial order parameter coset space. Note that both loops connect the same point due to the antipodal identification in this space.

Since smaller loops correspond to configurations with lower energy and higher order parameters, we can expect that if a loop *can* be contracted to a point then it will contract over time as the system equilibrates. Therefore, the contractible loops are unstable and disappear along with all of the integer defects, and the non-contractible loops remain stable along with their corresponding defect points. This fact about smaller loops also explains why we flip neighboring rods if their dot product is negative. That is, we do so in order to trace out the shortest possible loop in the order parameter coset space [9].

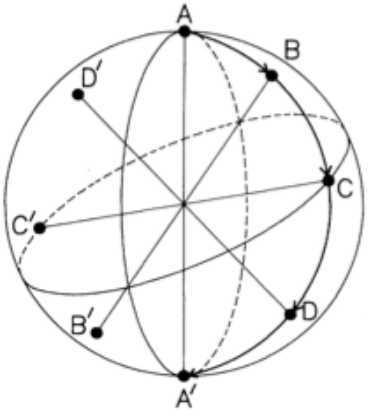

Figure 15: We choose the shortest path in OPC space by flipping neighboring rods that nearer antiparallel than parallel.

If the final dot product in the loop is negative, then the fourth and first molecules are closer to being antiparallel than they are to being parallel. This means that this loop is non-contractible in OPC space, and that it therefore contains a defect.

Once we have run the defect finding algorithm on the equilibrated system, we print the locations of the defects to Mathematica, where they are plotted within a 3 dimensional box representing the nematic cell. The presence of knotted defect structures is determined by visual examination of this 3D plot.

Using This Simulation to Create Knotted Structures

Unit Structures

Our first two approaches attempted to create a topologically stable structure that contained a unit knot. We will refer to this structure as a unit structure, since it could hypothetically be used to create a variety of different knots and links. Since the Backer Boundaries can predictably create 1/2-

integer disclinations perpendicular to the boundaries themselves, we attempt to create a unit structure with a unit knot surrounding a 1/2-integer defect line.

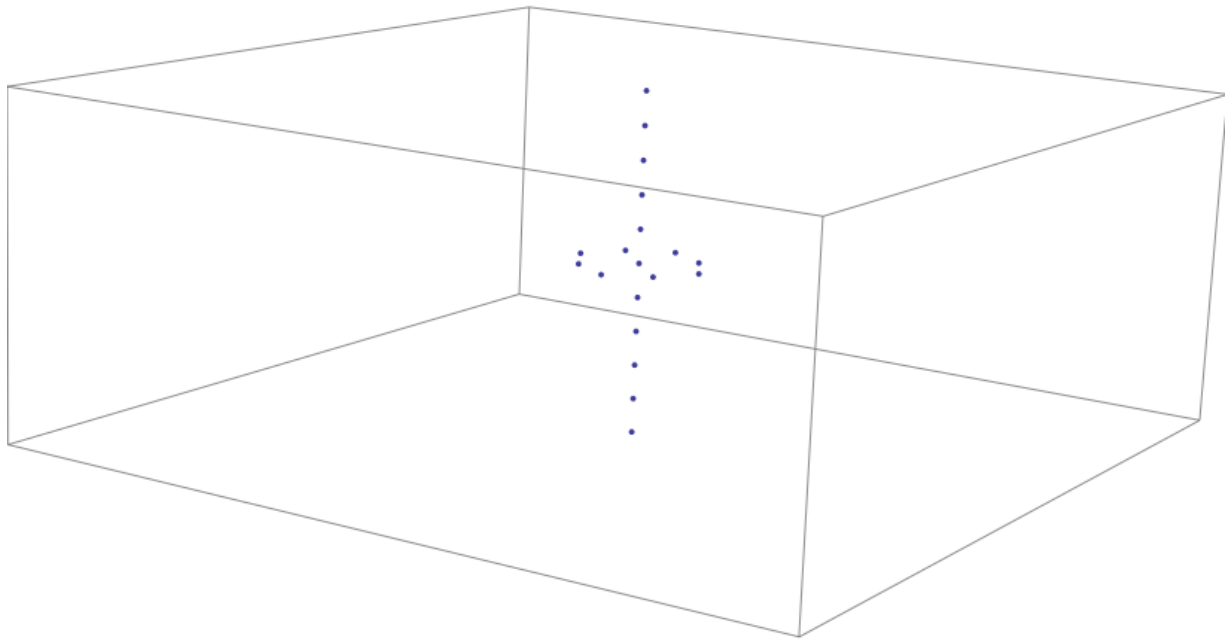

Figure 16: A topologically stable unit structure. It consists of a 1/2-integer disclination surrounded by an unknot.

Approach Using Orthogonal Pairs of Backer Boundaries

Our first approach in creating this unit structure utilized two pairs of Backer Boundaries, which are of course perpendicular to one another. We hypothesized that two 1/2-integer defect lines will form between each pair of boundaries.

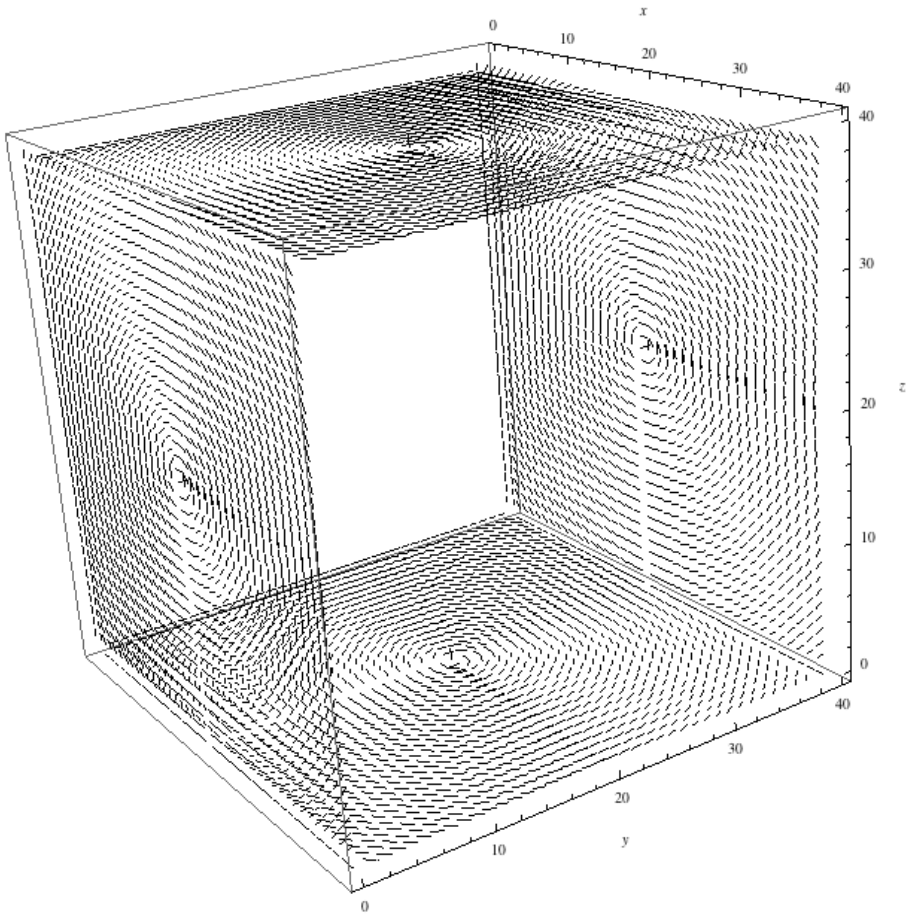

Figure 17: Two orthogonal pairs of Backer Boundaries.

We further hypothesized that it is possible to adiabatically move one pair of Backer Boundaries such that a one pair of lines is wrapped around the other. If the boundaries are shifted slowly enough such that the sample can re-equilibrate after each motion, we hypothesize that the neither pair of lines will dissipate.

If successful, then this approach would generate a unit structure which would then be stable with only a single pair of Backer Boundaries. Then the other pair could be removed and the process could be performed again.

Approach Using Wedge Disclination Loops

Our second approach for creating a unit structure utilizes Wedge Disclination Loops. As was previously stated, these loops form in the center of a sample with boundary molecules directed radially outward. Our approach is to create this stable loop and then rapidly change the boundaries parallel to the loop's plane to a pair of Backer Boundaries. If the loop is stable enough, we hypothesized that a 1/2-integer defect line would be driven through the loop, thereby creating a unit structure.

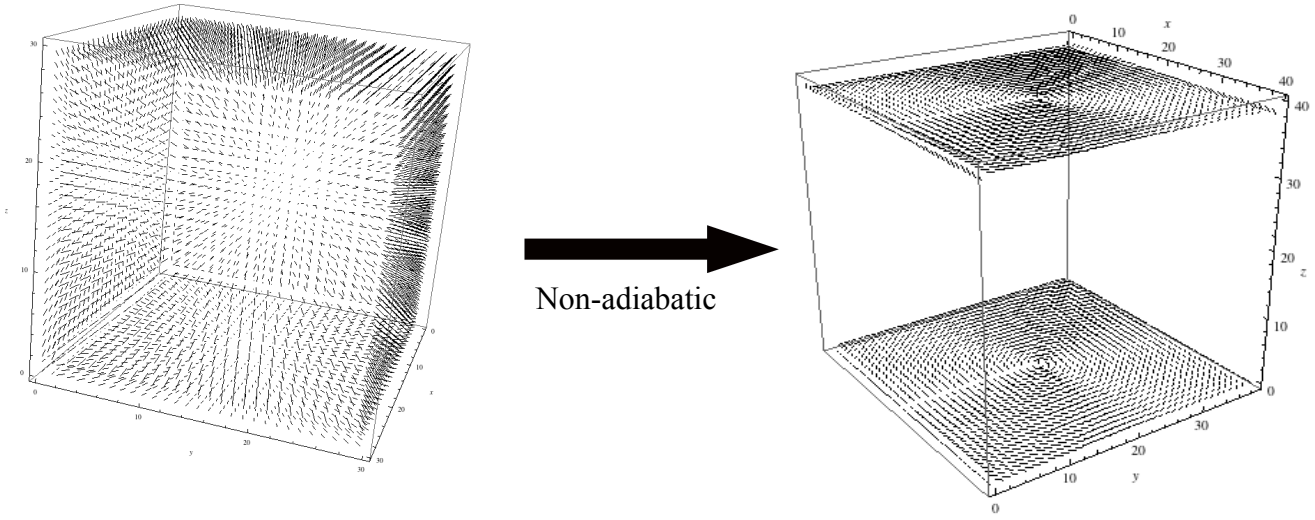

Figure 18: In this approach, we non-adiabatically switch to a pair of Backer boundaries (right) once the sample equilibrates under WDL boundaries (left)

In order to increase the stability of this loop, we apply a magnetic field perpendicular the loop's plane. This field couples to the molecules' orientations according to the formula:

$$Energy = -(\hat{H} \cdot \hat{n})^2$$

Where $\hat{n}$ is the local director and $\hat{H}$ is the magnetic field vector. This encourages the molecules to align perpendicular to loop's plane, which prolongs the loop's lifespan.

Approach Using Adiabatically Superimposed Backer Boundaries

This approach is unique in that it does not aim to create unit structures. Instead, with this approach we aim to create a Hopf Link, which is a structure with two unknots linked together once.

In this approach, we began with two standard Backer Boundaries on the “top” and “bottom” of the sample. Then we adiabatically introduced two more Backer Boundaries. One is slowly moved in on the top from the left, and the other is slowly moved in on the bottom from the right. We hypothesize that if these boundaries are introduced adiabatically, the original disclinations will not be disturbed. We also hypothesize that when the new Backer Boundaries' defects reach some critical distance from each other, another pair of 1/2-integer disclinations will be generated between them. We hypothesize that it is possible for the second set to form such that it is linked with the first set. If so, the boundaries can be eliminated and the linked structure will not dissipate, as it is topologically stable.

Results

Preliminary Results

We first demonstrate that the simulation reproduces well-understood results. These ensure that the simulation works correctly and reinforce the validity of any of this project's new results.

We first test the equilibration of a 3-D nematic with periodic, i.e. not fixed, boundary conditions. The scalar order parameter over time for this system is pictured below:

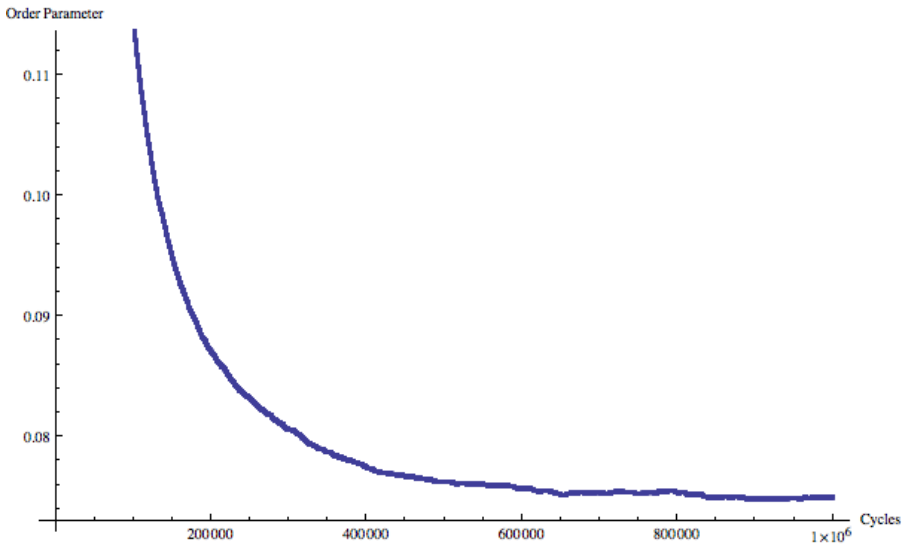

Figure 19: The scalar order parameter for an achiral nematic with periodic boundaries approaches a fixed value, as predicted.

Similar measures of the order parameter indicate that the following results also represent equilibrium states.

We then test the simulation's capability of reproducing a pair of Backer lines and a WDL. The boundaries and results are shown below:

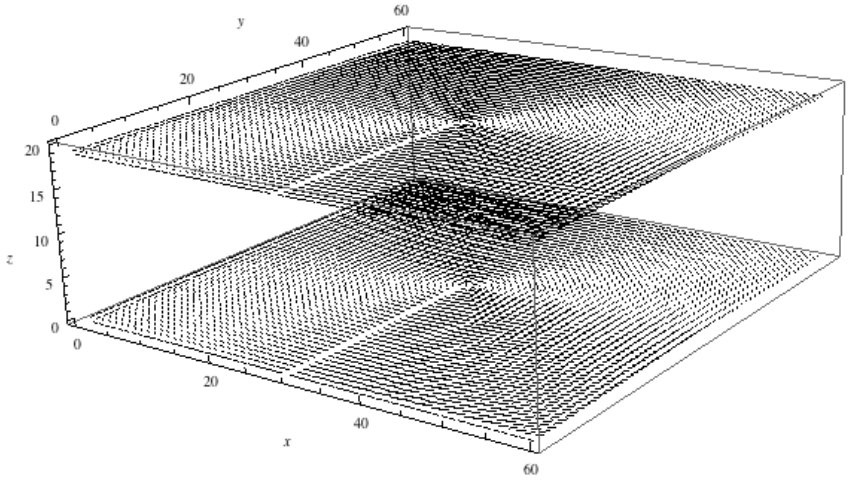

Figure 20: A single pair of Backer boundaries at z = 0 and z = 19 with length and width 60 were tested at T = 0.1. The defect structure in figure 21 formed after 1 billion Monte Carlo cycles.

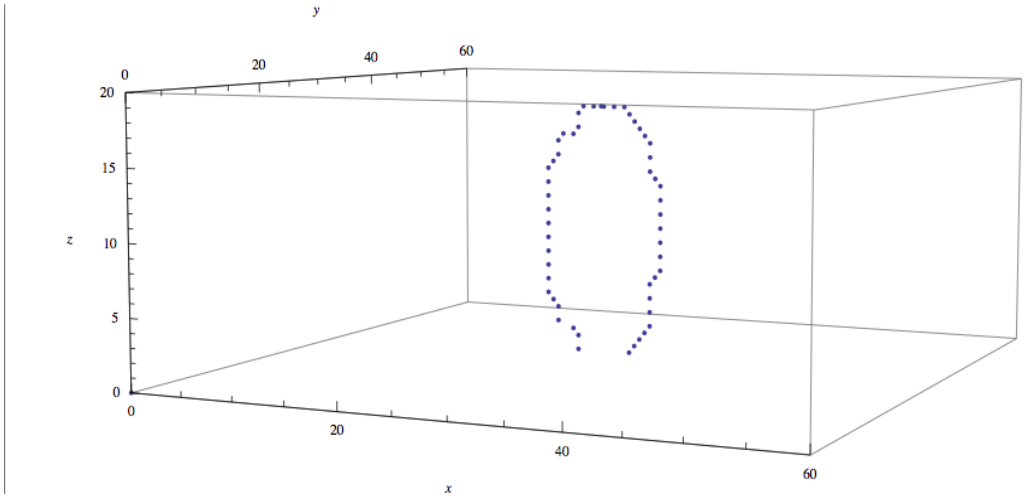

Figure 21: The Backer boundaries in figure 20 produced a single pair of Backer lines connecting the defects of strength -1 on each boundary. Each dot is a 1/2-integer defect, so each line is a 1/2-integer disclination.

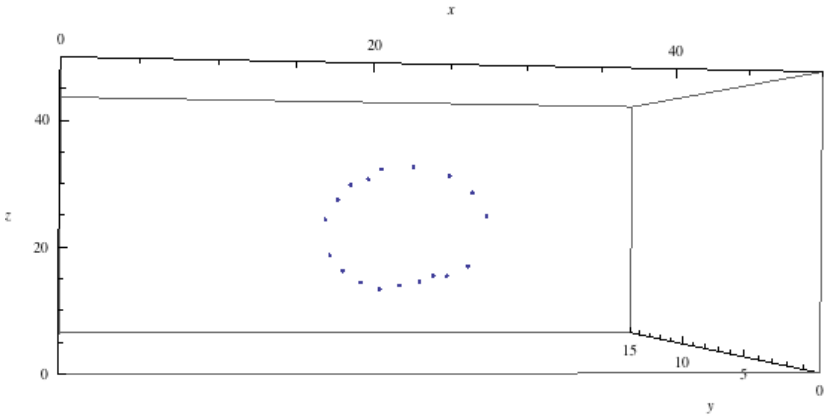

Figure 22: A cell with dimensions 50 x 15 x 50 (x,y,z) with WDL boundaries successfully produces a wedge disclination loop.

Orthogonal Backer Boundaries

The orthogonal Backer boundaries approach failed to produce unit defect structures. The results were dependent on the dimensions of the sample.

For samples with one square pair and one rectangular pair of boundaries, disclinations formed immediately underneath fixed Backer boundaries and ran diagonally from one +1 defect to another, as in Backer's results [6]. We found similar results for samples with unequal length, width, and height.

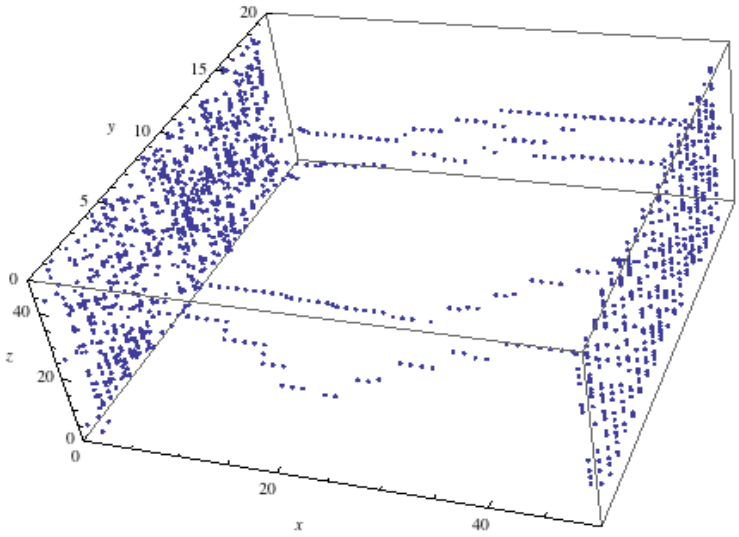

Figure 23: 1/2-integer disclinations form immediately underneath fixed single cell Backer boundaries.

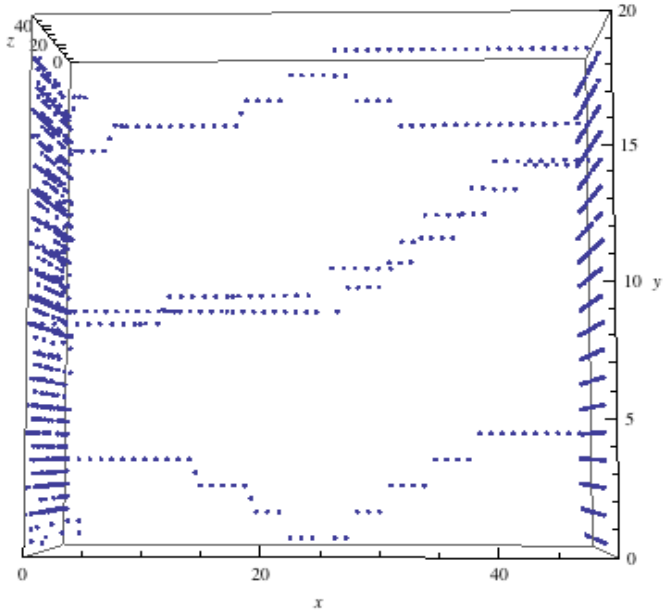

Figure 25: The same result as figure 24, but viewed from the above.

Analysis

We found that disclinations could not be reliably formed between -1 defects on opposing Backer boundaries when multiple pairs of Backer boundaries were used. Therefore, it would not be possible to

adiabatically move the disclinations such that a unit structure could be formed. As such, the orthogonal Backer boundary approach is unsuitable for the generation of unit structures.

WDL

The WDL approach also failed to produce unit defect structures. In every simulation, the WDL disintegrated too quickly after switching to Backer boundary conditions. This process was delayed by applying a magnetic field, but not by a significant amount. Below are typical results without and with an applied magnetic field.

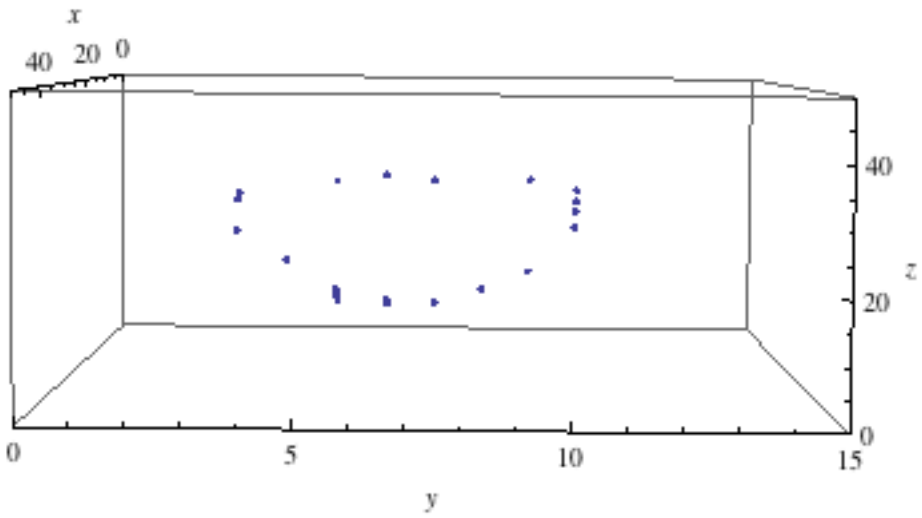

Figure 26: An example of WDL disintegration in a 50-15-50 cell with no magnetic field applied. Here, the WDL has stabilized after 700 million Monte Carlo cycles.

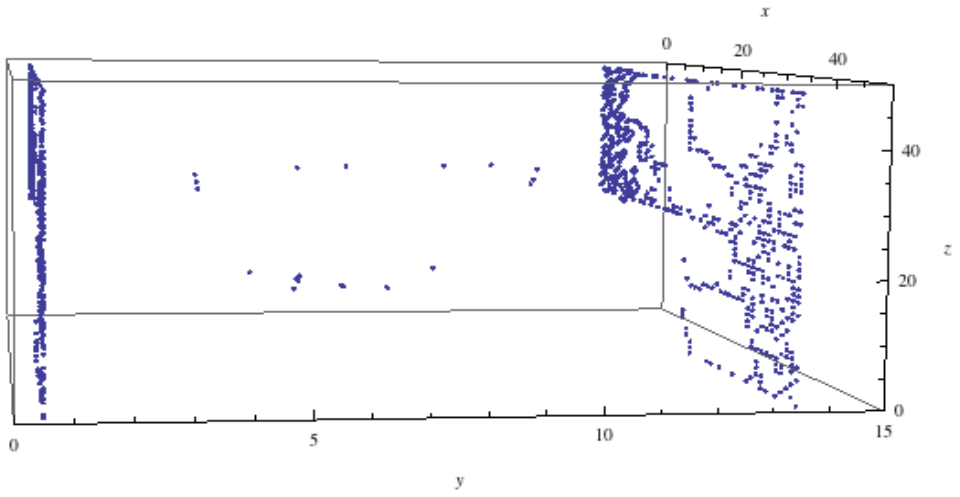

Figure 27: The defect structure immediately (1 cycle) after switching to Backer boundaries. Note that the defects are located mostly near the non-Backer boundaries.

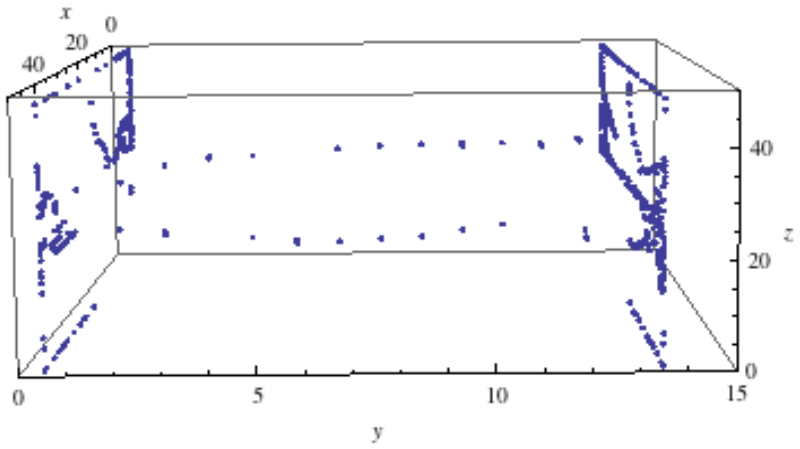

Figure 28: The WDL has begun to disintegrate 90 million cycles after the switch to Backer boundaries on the yz planes. Note that it has not maintained the unknot's topology.

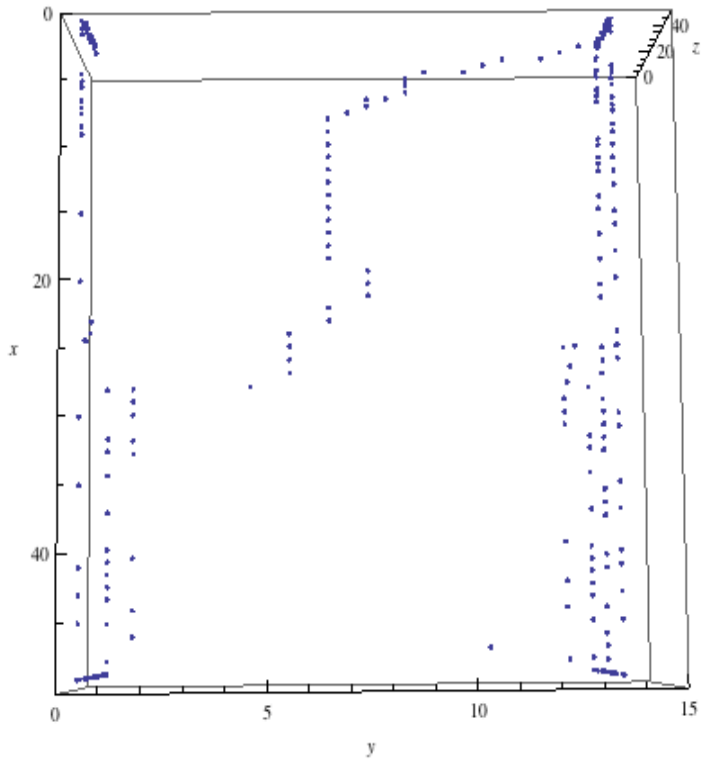

Figure 29: The near-equilibrium state for this system as viewed from the top. Note that the WDL has completely disappeared 130 million cycles after switching to Backer boundaries.

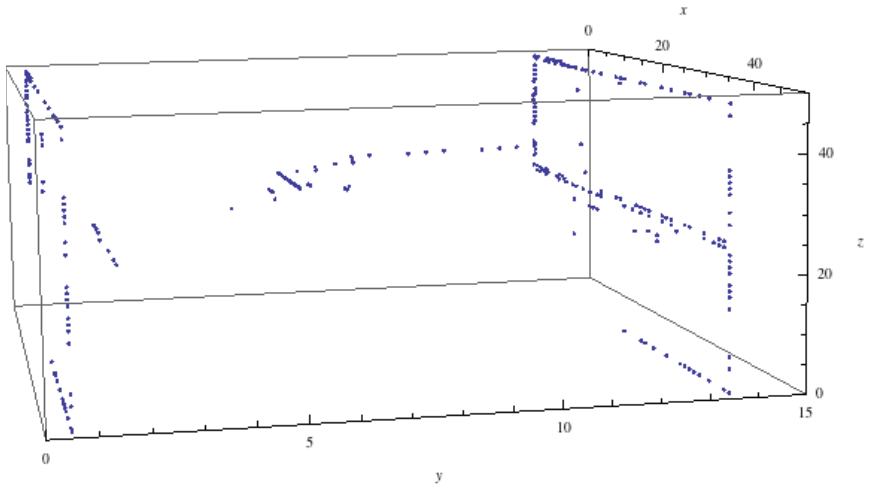

Figure 30: The near-equilibrium state for this system as viewed from the side. A disclination connects diagonally opposite points on the z = 25 plane.

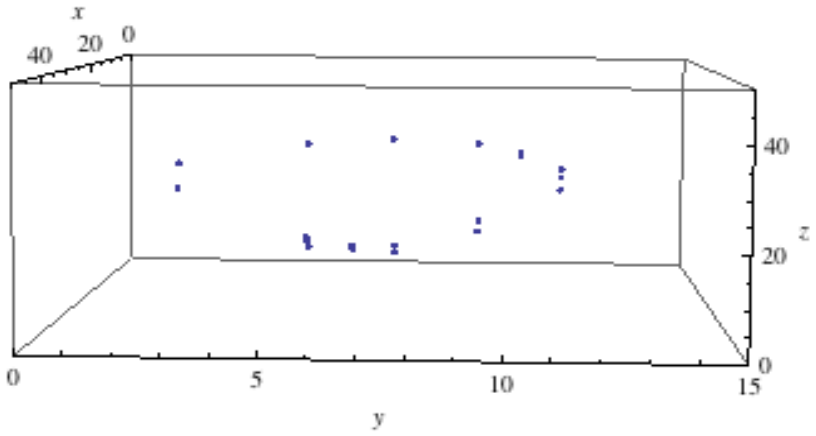

Figure 31: This simulation the same configuration as the previous figures, but has a magnetic field H = 0.05. We see that WDL formation is not impaired after 700 million cycles.

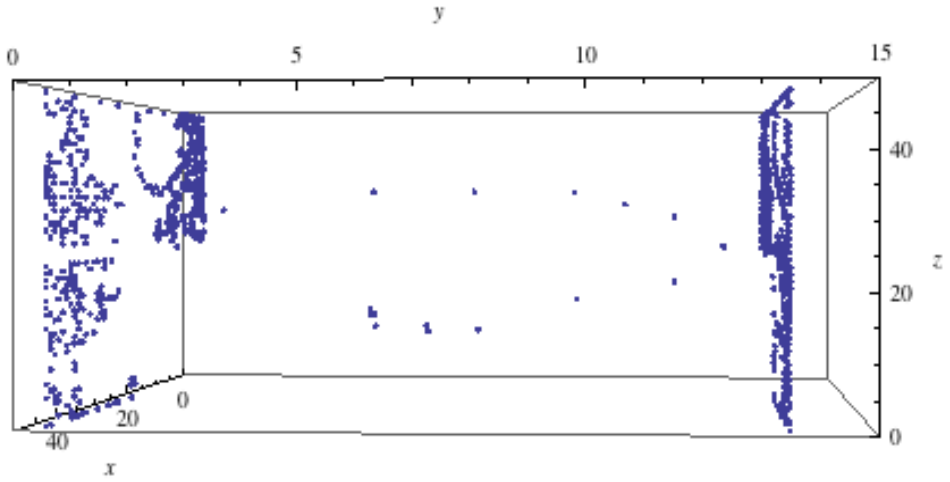

Figure 32: The defect profile 1 cycle switching to Backer boundaries. Note that the WDL has already begun to disintegrate.

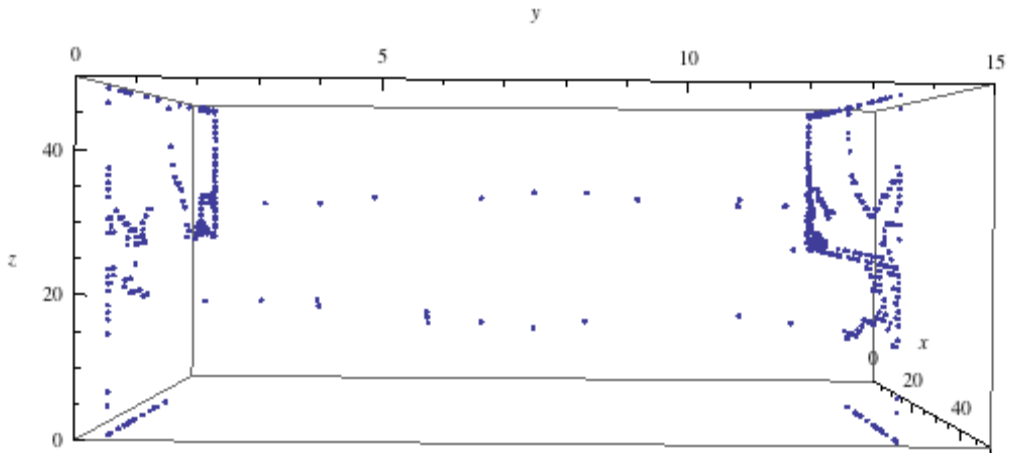

Figure 33: Despite the magnetic field, we observe the same behavior 90 million cycles after switching to Backer boundaries.

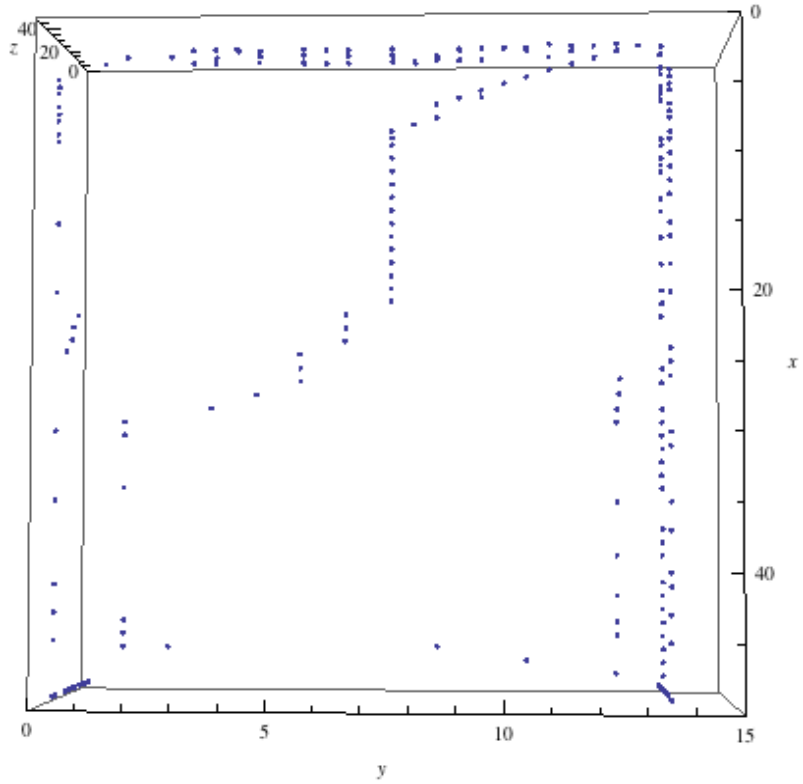

Figure 34: Despite the magnetic field, we observe a similar near-equilibrium configuration of this sample. Again, the WDL has entirely dissipated before it could be used to create a unit structure.

Analysis

The two above experiments illustrate typical results for the WDL approach. At strengths where it did not disrupt the formation of the WDL, the magnetic field was not helpful in extending the WDL's lifespan. After approximately 90 million cycles, the WDL completely failed to preserve its topology. Therefore, our hypothesis was incorrect due to the severity of the WDL's instability. As such, the WDL approach is not a viable hod for generating unit structures.

Hopf Link

Parameters that were adjusted for different simulations included the speed at which new boundaries were introduced, the direction from which they were introduced, and if they were introduced one row at a time or with multiple rows at once. Despite the many variations of this approach that were used, we were unable to find its stable equilibrium structures. All available data is chaotic and demonstrates no discernible pattern. Therefore, we classify the results of this approach as inconclusive and conjecture that it is unlikely to produce knotted defect structures.

Conclusion

Knotted defect structures are novel and fascinating structures that can appear in liquid crystals under appropriate conditions. However, they are difficult to create and manipulate using current methods. This project investigated the possibility of creating knotted defect structures using only boundary conditions. A boundary condition method would be easy to simulate and also to implement experimentally. Their ease of use and flexibility in application was the primary motivation for studying their capacity to generate knotted defect structures.

Three approaches were used in this project. The first two attempted to generate a topologically stable structure that included a unit knot, which could be used as a basic building block for more

complicated knots and links. The third approach attempted to generate a Hopf Link, the simplest non-trivial link.

The current evidence indicates that all three approaches are not viable candidates for the generation of knotted defect structures via boundary conditions. However, this does not rule out the possibility that boundary conditions could be used towards this end. There are many other boundary conditions and possible combinations of boundary conditions that were not tested in this project. Therefore, the question of whether or not knotted defect structures can be created solely with boundary conditions is still open. However, the results of this project indicate that approaches using unit structures are likely unfavorable. Instead, future simulations should be geared towards generated already-linked structures (e.g. Hopf Links). Future investigations should also consider using chiral nematic liquid crystals, whose capacity for creating unit or pre-linked structures was not considered in this project.

Bibliography

1. http://upload.wikimedia.org/wikipedia/commons/c/ce/Hopf_Link.png
2. Collings, Peter J. Liquid Crystals: Nature's Delicate Phase of Matter. 2002. Princeton University Press
3. Shukla, Prabodh. Physics of Disordered Solids. 1981. Mittal Publications.
4. http://wpcontent.answcdn.com/wikipedia/commons/thumb/3/37/Blue_Unknot.png/150px-Blue_Unknot.png
5. http://mathworld.wolfram.com/images/eps-gif/ReidemeisterMoves_1001.gif
6. Backer, A. , Callan-Jones A.C. , Pelcovits, R. Physical Review E. **77.** 021701. (2008)
7. Crompton, Octavia. Monte Carlo Simulation of a 2-Dimensional Lebwohl-Lasher Model. Brown University Physics Department. (2010).
8. Mermin, N.D. The Topological Theory of Defects in Ordered Media. Reviews of Modern Physics, Vol. 51, No. 3, July 1979.
9. Zapotocky, M., Goldbart, P. , Goldenfeld, N. Kinetics of Phase Ordering in Uniaxial and Biaxial Nematic Films. Physical Review E. Vol. 51, No. 2, February 1995.
10. Witten, Edward. Knots and Quantum Theory. The Institute Letter, Spring 2011.
11. Bausch, A., Schaller, V. A Fresh Twist for Self-Assembly. Nature Materials Science, 2012.
12. Ravnik M. et al. Entangled Nematic Colloidal Dimers and Wires. Physics Review Letters, December 2007.
13. Schwarz, M. and Pelcovits, R. Nematic Cells with Quasicrystalline-patterned Alignment Layers. Physical Review E, February 2009.
14. Kaplan, C., Tu H, Pelcovits, R., Meyer, R. Theory of Depletion Induced Phase Transition from Chiral Smectic-A Twisted Ribbons to Semi-Infinite Flat Membranes. Physical Review E, August 2010.

15. Yang, Y. et al. Self-Assembly of 2D Membranes from Mixtures of Hard Rods and Depleting Polymers. Soft Matter, 2012, **8**, 707.

16. Stephen, M., Straley, J. Physics of Liquid Crystals. Reviews of Modern Physics, Vol. 46, No. 4, October 1974.

17. Tkalec, U. et al. Reconfigurable Knots and Links in Chiral Nematic Colloids. Science, Vol 333, July 1, 2011.

18. Terentjev, E. Disclination Loops, Standing Alone and Around Solid Particles, in Nematic Liquid Crystals. Physical Review E, Vol. 51, No.2, February 1995.

19. Prasolov, V. Knots, Links, Braids, and 3-Manifolds: An Introduction to the New Invariants in Low-Dimensional Topology. American Mathematical Society. October 15, 1996.